

MODELLING FOR ENGINEERING & HUMAN BEHAVIOUR 2019

im²

Instituto Universitario de Matemática Multidisciplinar
Polytechnic City of Innovation

Edited by

R. Company, J.C. Cortés,
L. Jódar and E. López-Navarro

July 10th - 12th 2019



UNIVERSITAT
POLITÈCNICA
DE VALÈNCIA



CIUDAD POLITÈCNICA
DE LA INNOVACIÓN



Modelling for Engineering & Human Behaviour 2019

València, 10 – 12 July 2019

This book includes the extended abstracts of papers presented at XXIst Edition of the Mathematical Modelling Conference Series at the Institute for Multidisciplinary Mathematics “Mathematical Modelling in Engineering & Human Behaviour”.

I.S.B.N.: 978-84-09-16428-8

Version: 15/11/19

Report any problems with this document to ellona1@upvnet.upv.es.

Edited by: R. Company, J. C. Cortés, L. Jódar and E. López-Navarro.

Credits: The cover has been designed using images from [kjpargeter/freepik](https://www.kjpargeter.com/).

im²

Instituto Universitario de Matemática
Multidisciplinar

This book has been supported by the European Union through the Operational Program of the [European Regional Development Fund (ERDF) / European Social Fund (ESF)] of the Valencian Community 2014-2020. [Record: GJIDI/2018/A/010].



Fons Europeu de
Desenvolupament Regional

Una manera de fer Europa

Contents

A personality mathematical model of placebo with or without deception: an application of the Self-Regulation Therapy	1
The role of police deterrence in urban burglary prevention: a new mathematical approach	9
A Heuristic optimization approach to solve berth allocation problem	14
Improving the efficiency of orbit determination processes	18
A new three-steps iterative method for solving nonlinear systems	22
Adaptive modal methods to integrate the neutron diffusion equation	26
Numerical integral transform methods for random hyperbolic models	32
Nonstandard finite difference schemes for coupled delay differential models	37
Semilocal convergence for new Chebyshev-type iterative methods	42
Mathematical modeling of Myocardial Infarction	46
Symmetry relations between dynamical planes	51
Econometric methodology applied to financial systems	56
New matrix series expansions for the matrix cosine approximation	64
Modeling the political corruption in Spain	70
Exponential time differencing schemes for pricing American option under the Heston model	75
Chromium layer thickness forecast in hard chromium plating process using gradient boosted regression trees: a case study	79
Design and convergence of new iterative methods with memory for solving nonlinear problems	83
Study of the influence falling friction on the wheel/rail contact in railway dynamics ..	88
Extension of the modal superposition method for general damping applied in railway dynamics	94
Predicting healthcare cost of diabetes using machine learning models	99

Sampling of pairwise comparisons in decision-making	105
A multi-objective and multi-criteria approach for district metered area design: water operation and quality analysis	110
Updating the OSPF routing protocol for communication networks by optimal decision-making over the k-shortest path algorithm	118
Optimal placement of quality sensors in water distribution systems	124
Mapping musical notes to socio-political events	131
Comparison between DKGa optimization algorithm and Grammar Swarm surrogated model applied to CEC2005 optimization benchmark	136
The quantum brain model	142
Probabilistic solution of a randomized first order differential equation with discrete delay	151
A predictive method for bridge health monitoring under operational conditions	155
Comparison of a new maximum power point tracking based on neural network with conventional methodologies	160
Influence of different pathologies on the dynamic behaviour and against fatigue of railway steel bridges	166
Statistical-vibratory analysis of wind turbine multipliers under different working conditions	171
Analysis of finite dimensional linear control systems subject to uncertainties via probabilistic densities	176
Topographic representation of cancer data using Boolean Networks	180
Trying to stabilize the population and mean temperature of the World	185
Optimizing the demographic rates to control the dependency ratio in Spain	193
An integer linear programming approach to check the embodied CO_2 emissions of the opaque part of a façade	199
Acoustics on the Poincaré Disk	206
Network computational model to estimate the effectiveness of the influenza vaccine <i>a posteriori</i>	211

Acoustics on the Poincaré Disk

Michael M. Tung ^{b1}

(b) Instituto de Matemática Multidisciplinar,
Universitat Politècnica de València.

1 Introduction

The Poincaré disk model is a straightforward model of hyperbolic geometry [1] on the 2-dimensional disk taking over certain properties from the Poincaré half-plane [2, 3]. The corresponding metric of this manifold weighs radial distances from the center of the disk to its circumference in a characteristic manner. Not only from the mathematical viewpoint has this model fundamental relevance, but we will argue that its prominent feature can be interpreted as somewhat that of a black hole turned upside down, a quality absent from the related half-plane analogue [4]. This particular geometry and topology make it an attractive candidate for acoustic wave simulation with metamaterial devices—devices composed of extraordinary materials which allow to implement curved background spacetimes in acoustics, see [5–9] and references therein.

In this work we study the feasibility to implement acoustics on the Poincaré disk and investigate the wave propagation in such a medium. We explore the main differential-geometric features of this spacetime with its asymptotic behaviour and causal boundaries very much alike to those of acoustic black holes [9]. By employing the framework developed in [6, 7] we find the acoustic laboratory parameters (mass-density tensor and bulk modulus) corresponding to the underlying spacetime structure. We also derive the equations of motion which govern acoustic wave propagation on the Poincaré disk. This work concludes with numerical simulations for one illustrative example.

2 Spacetime geometry

The Poincaré disk, henceforth denoted by \mathbb{D}_P , is the resulting image of the stereographic projection $(X, Y, Z) \mapsto (x, y)$ of the upper part of a circular hyperboloid of two sheets, represented by the equation $X^2 + Y^2 - Z^2 = -a^2$, onto the xy -plane.

Fig. 1 provides a schematic view of the stereographic mapping, and shows the similar triangles to yield the following relations between the coordinates of the hyperboloid and its projection

¹e-mail: mtung@imm.upv.es

to the plane, *i.e.*

$$\frac{x}{a} = \frac{X}{Z+a}, \quad \frac{y}{a} = \frac{Y}{Z+a}. \quad (1)$$

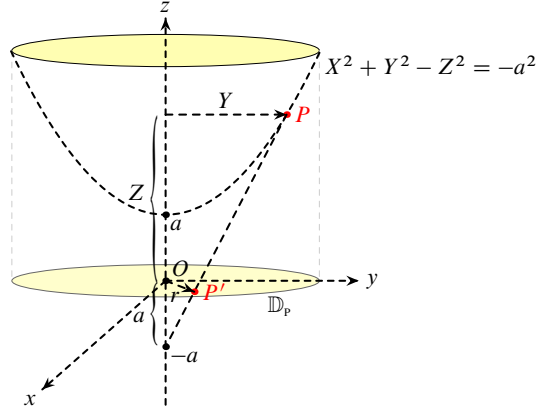


Figure 1: Schematic view of the stereographic projection of point P on the upper sheet of a circular hyperboloid to point P' located on the plane $z = 0$. The projection gives the Poincaré disk, \mathbb{D}_P , endowed with a characteristic metric.

Using the conventional radial polar coordinate r on the xy -plane, it is not difficult to find

$$\left. \begin{aligned} X &= \frac{2x}{1 - r^2/a^2} \\ Y &= \frac{2y}{1 - r^2/a^2} \\ Z &= \frac{1 + r^2/a^2}{1 - r^2/a^2}a \end{aligned} \right\} \text{ for } 0 \leq r < a, \quad (2)$$

This induces the following spatial line element for distances ℓ on Poincaré disk \mathbb{D}_P :

$$d\ell^2 = dX^2 + dY^2 = 4 \frac{dx^2 + dy^2}{(1 - r^2/a^2)^2}. \quad (3)$$

Now, it is customary to introduce the geodesic radius $\varrho = \text{artanh}(r/a)$, which converts (3) to the much simpler form

$$d\ell^2 = a^2 d\varrho^2 + a^2 \sinh^2 \varrho d\varphi^2. \quad (4)$$

Note that (4) represents the metric of hyperbolic geometry underlying much of the famous artwork by the Dutch artist M.C. Escher [10]. Then, adding the time component, the full spacetime metric for the Lorentzian manifold $M = \mathbb{D}_P \times \mathbb{R}$ is given by

$$\mathbf{g} = -(\underbrace{cdt}_{\theta^0}) \otimes (\underbrace{cdt}_{\theta^0}) + (a d\varrho) \otimes (\underbrace{a d\varrho}_{\theta^1}) + (a \sinh \varrho d\varphi) \otimes (\underbrace{a \sinh \varrho d\varphi}_{\theta^2}), \quad (5)$$

where θ^μ ($\mu = 0, 1, 2$) indicates the dual-base forms of the local coframe. Recall that $a > 0$ is a physical length scale, further ϱ and φ are geodesic polar coordinates. Moreover, $c > 0$ is a constant speed. This completes the spacetime setup necessary for the succeeding wave simulation.

3 Physical construction

In combination with Cartan's structure equations, the dual base $\{\theta^0, \theta^1, \theta^2\}$ introduced by (5) allows to straightforwardly compute the Riemann curvature tensor $\hat{R}^\alpha_{\beta\gamma\delta}$ in the coframe of manifold $M = \mathbb{D}_p \times \mathbb{R}$. The only non-zero and independent component turns out to be

$$\hat{R}^1_{212} = -\frac{1}{a^2} \quad \Rightarrow \quad G_{00} = \hat{G}_{00} = -\frac{1}{a^2}. \quad (6)$$

In the final step of (6), we have given the corresponding Einstein tensor $\hat{G}_{\alpha\beta}$, whose 00-components in the local coframe and coordinate frame are identical. As an immediate consequence of (6) the underlying energy-matter density ρ_0 is exotic:

$$\underbrace{G_{00}}_{-1/a^2} = \frac{8\pi G}{c^4} \underbrace{T_{00}}_{\rho_0 c^2} \quad \Rightarrow \quad \rho_0 = -\frac{c^2}{8\pi G a^2} < 0, \quad (7)$$

where G is the usual gravitational constant. As expected, if the disk extends to infinity, *viz.* $a \rightarrow \infty$, the energy-matter content will vanish and M becomes asymptotically flat.

Obviously, current—and likely any future technology—does not permit to implement such physical configuration with negative energy-matter density. However, fine-tuning the acoustic parameters of a suitable metamaterial will presumably allow to do so in the near future. In Ref. [7], we have shown that there exists a general 1-to-1 correspondence between spacetime metric \mathbf{g} and the parameters κ (bulk modulus) and $\boldsymbol{\rho}$ (density tensor) of an acoustic metamaterial device. In this case, using (5), we obtain for $0 \leq r < a$:

$$\kappa = \frac{4}{(1 - r^2/a^2)^2} \kappa_0, \quad \rho_0 \rho^{ij} = \frac{1}{4} (1 - r^2/a^2)^2 \begin{pmatrix} 1 & 0 \\ 0 & 1 \end{pmatrix}. \quad (8)$$

Note that the constants κ_0 and ρ_0 are fixed by the physical properties of the corresponding flat space. This completes the implementation of the Poincaré disk $M = \mathbb{D}_p \times \mathbb{R}$ for metamaterial acoustics.

4 Wave simulation

Once the acoustic metamaterial is configured, wave propagation can be simulated in such media. Acoustic phenomena will be governed by an elementary variational principle, namely that for a spacetime M , endowed with metric \mathbf{g} , the action will be stationary with respect to variations of the acoustic potential $\phi : M \rightarrow \mathbb{R}$, such that integration over bounded spacetime domain $\Omega \subseteq M$ with volume element $d\text{vol}_g$ satisfies [7]:

$$\frac{\delta}{\delta\phi} \int_{\Omega} d\text{vol}_g \mathbf{g}(\nabla\phi, \nabla\phi) = 0. \quad (9)$$

Next, the variational principle, (9), amounts to solving

$$*d*d\phi = 0, \quad (10)$$

where $*$ is the Hodge dual. In local coordinates, (10) takes the form of the wave equation with the Laplace-Beltrami Δ_M operator for the curved spacetime background M .

To take advantage of the underlying rotational symmetry, we choose concentric waves centered around the origin for acoustic probing. Then, all non-trivial behaviour of the acoustic potential ϕ is contained in a radial factor, which we denote by $\phi_1(\varrho)$. Furthermore, considering rotational symmetry, we can show that the exact solutions for $\phi_1(\varrho)$, satisfying (10), are combinations of Legendre polynomials with complex arguments.

Apart from the exact result, we have derived a relatively simple and accurate approximate solution for the radial dependence of the potential:

$$\phi_1(\varrho) = e^{-\varrho/2} \left[A e^{\sqrt{1-4a^2\omega^2/c^2}\varrho} + B e^{-\sqrt{1-4a^2\omega^2/c^2}\varrho} \right]. \quad (11)$$

Here, ω specifies the frequency of the monochromatic sound waves, and A and B are constants determined by the boundary conditions. Extreme damping occurs in the asymptotic limit $\varrho \rightarrow \infty$ ($r \rightarrow a$), and consequently it will never be possible to escape \mathbb{D}_p . Moreover, oscillatory behaviour emerges when $\omega > \frac{c}{2a}$. For a numerical simulation, we assume $a = 1$, $c = 1$, and $\omega = 1 > 1/2$, so that naturally harmonic wave features will materialize. Fig. 2 captures exact and approximate results for the boundary conditions $\phi_1(1) = 1$ and $\phi_1'(1) = 0$. The absolute error is exceptionally good and ranges between $2.65 \cdot 10^{-8}$ and 0.018 (only close to $\varrho = 3.4$).

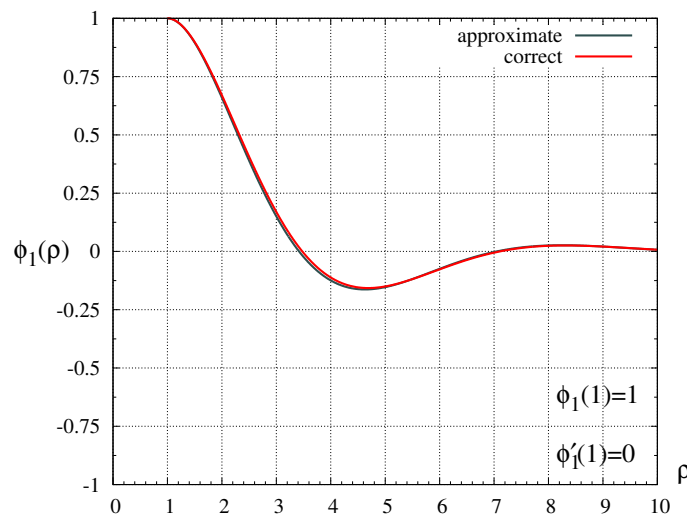


Figure 2: Non-trivial radial dependence of the acoustic potential for scale $a = 1$, speed $c = 1$, frequency $\omega = 1$, with conditions $\phi_1(1) = 1$, $\phi_1'(1) = 0$.

References

- [1] Anderson, J.W., *Hyperbolic Geometry*. Berlin, Springer-Verlag, 2005.
- [2] Kelly, P.J. and Matthews, G., *The Non-Euclidean Hyperbolic Plane: Its Structure and Consistency*. Berlin, Springer-Verlag, 1981.

- [3] Stahl, S., *A Gateway to Modern Geometry: The Poincaré Half-Plane*. Burlington, MD, Jones & Bartlett, 2008.
- [4] Tung, M.M., Modelling acoustics on the Poincaré half-plane, *J. Comput. Appl. Math.*, 337: 336–372, 2018.
- [5] Cummer, S., A sound future for acoustic metamaterials, *J. Acoust. Soc. Am.*, 141(5): 3451, 2017.
- [6] Tung, M.M. and Peinado, J., A covariant spacetime approach to transformation acoustics. *Progress in Industrial Mathematics at ECMI 2012*, M. Fontes, M. Günther, N. Marheineke, (eds.), Mathematics in Industry, 19: 335–340, 2014.
- [7] Tung, M.M., A fundamental Lagrangian approach to transformation acoustics and spherical spacetime cloaking, *Europhys. Lett.*, 98: 34002–34006, 2012.
- [8] Tung, M.M. and Weinmüller, E.B., Gravitational frequency shifts in transformation acoustics, *Europhys. Lett.*, 101: 54006–54011, 2013.
- [9] Tung, M.M. and Weinmüller, E.B., Acoustic metamaterial models on the (2+1)D Schwarzschild plane, *J. Comput. Appl. Math.*, 346: 162–170, 2019.
- [10] Schattschneider, D., The mathematical side of M.C. Escher, *Notices Am. Math. Soc.*, 57(6): 706–718, 2010.